Current Chemistry Letters 12 (2023) 445–458

Contents lists available atGrowingScience

Current Chemistry Letters

homepage: www.GrowingScience.com

Studies of kinetic models and adsorption isotherms: application on the interaction of insulin with synthetic hydroxyapatite

Abdelhadi El Rhilassi[a*] and Mounia Bennani Ziatni[a]

[a]*Laboratory of Organic Chemistry, Catalysis and Environment, Department of Chemistry, Faculty of Sciences, Ibn Tofail University, BP 242, 14000, Kenitra, Morocco*

C H R O N I C L E

Article history:
Received May 23, 2022
Received in revised form
June 25, 2022
Accepted October 21, 2022
Available online
October 21, 2022

Keywords:
Hydroxyapatite
Insulin
Langmuir
Pseudo second order

A B S T R A C T

The non-stoichiometric, calcium-deficient hydroxyapatite was prepared through a low-temperature from aqueous solutions method and characterized using Physico-chemical methods. The potential of this hydroxyapatite to adsorb and release insulin from aqueous solutions was evaluated under physiological conditions. The effect of contact time and initial concentration were studied in batch experiments. The adsorption rate reached up to 81±5% in the first half-hour of contact, while the release rate of insulin incubation was about 41 ± 5% after 1 hour. The pseudo-first-order, pseudo-second-order, Elovich equation, Weber and Morris intraparticle diffusion model and Bangham's pore diffusion model were applied to study the kinetics of the adsorption process. The pseudo-second-order kinetic model provided the best correlation $R^2(0.998)$ of the used experimental data compared to the other models. The adsorption of insulin onto hydroxyapatite was correlated well $R^2(0.998)$ with the Langmuir model as compared to Freundlich, Temkin and Dubinin–Kaganer–Radushkevich (D-K-R) models, with a maximum adsorption capacity of 24.46 mg/g. The isotherms parameters values of ΔG^0, b_t and E *show* that the adsorption process is favorable, spontaneous, exothermic, and controlled by physisorption. The point of zero charge (pH_{ZPC}) of hydroxyapatite and the isoelectric point (pI) of insulin indicate that the interaction of insulin molecules with prepared apatite can be well described as an ions exchange reaction.

1. Introduction

Nowadays, it is interesting to say that organic and inorganic compounds have a lot of useful applications and this advantage was shown in a lot of papers published before.[1-7] In recent years, studies of the adsorption and release of bioactive molecules and proteins have been carried out on synthetic calcium phosphate apatites.[8,9]

Due to the similarity to bone mineral, hydroxyapatite (HA) is one of the most important apatites for dental and biomedical applications such as drug delivery systems and bone reconstruction.[10-12] HA can be considered an excellent biocompatible, bioactive, and osteoconductive.[13] Several techniques have been used for the preparation of hydroxyapatite such as low-temperature chemical solution methods,[14] and high-temperature solid-state reactions.[15] In this paper, the poorly crystalline hydroxyapatite was synthesized at low temperatures (298 K) and at neutral pH.

Generally, the stoichiometric hydroxyapatite (HA) of Ca/P =1.67 has a formula $Ca_{10}(PO_4)_6(OH)_2$, their pH stability range in aqueous solutions is between 6.5–9.5 at 298 K.[16] The non-stoichiometric, calcium-deficient hydroxyapatite (CDHA) with Ca/P ratio within 1.5–1.67,[17] is described by the following formula $Ca_{10-x}(PO_4)_{6-x}(HPO_4)_x(OH)_{2-x}$ with $0 < x$

* Corresponding author. Tel : +212 6 62 13 13 72
E-mail address aelrhilassi@gmail.com (A. El Rhilassi)

doi: 10.5267/j.ccl.2022.11.001

≤ 1,[18] their pH stability in aqueous (298 K) is between 9.5–12.[16] It's interesting to note that the chemical *formula* of CDHA is composed of HPO_4^{2-} anions and has vacant Ca^{2+} sites, which suggests the greater reactivity of these apatitess with active molecules such as amino acids and insulin.

One of the most important factors in understanding the adsorption process is predicting the rate of the kinetics of the reaction of this process and also its step of limiting. Therefore, it is necessary to determine the rate-limiting step which governs the overall adsorption rate and its mechanism.

In this paper, we are interested in studying the interaction of insulin with synthetic poorly crystalline calcium-deficient hydroxyapatite. For this reason, the kinetic models and the adsorption isotherms models are applied in order to analyze successfully the adsorption of insulin on the CDHA and determine the best mathematical model fitting with experimental data.

2. Material and methods

2.1 Adsorbate

Human insulin is a simple protein consisting of two chains having 21 and 30 amino acids. The chains are joined together by two disulfide bonds. The active substance is produced in the laboratory by recombinant DNA technology. In this study, the human insulin tested is from Novo Nordisk A/S (Bagsvaerd, Denmark). The samples of adsorbate are prepared from a stock solution of 3500 mg/l using physiological saline (NaCl 9g/l). The most important physicochemical properties of human insulin are collected in table1. The FT-IR spectrum of human insulin (**Fig.1**) reveals the presence of characteristic absorption bands of insulin, one at 3398.9 cm^{-1} attributed to the stretching vibration of the NH_2 group,[19] and others at 1658.3 cm^{-1}, 1516.4cm^{-1}, and 1240.6 cm^{-1} corresponds respectively to the amide I, amide II and amide III, mainly due to C=O stretching vibration.[20]

Table 1. Physicochemical properties of human insulin.

Name	human insulin
Molecular formula	$C_{257}H_{383}N_{65}O_{77S6}$
Molecular weight	5808
Condensed Structural formula according to International Union of Pure and Applied Chemistry (IUPAC)	H-Phe-Val-Asn-Gln-His-Leu-Cys(1)-Gly-Ser-His-Leu-Val-Glu-Ala-Leu-Tyr-Leu-Val-Cys(2)-Gly-Glu-Arg-Gly-Phe-Phe-Tyr-Thr-Pro-Lys-Thr-OH. H-Gly-Ile-Val-Glu-Gln-Cys(3)-Cys(1)-Thr-Ser-Ile-Cys(3)-Ser-Leu-Tyr-Gln-Leu-Glu-Asn-Tyr-Cys(2)-Asn-OH
Isoelectric point (pI)	5.4
Storage temperature	2° - 8°C
Shelf-life of the substance	Up to 2 years

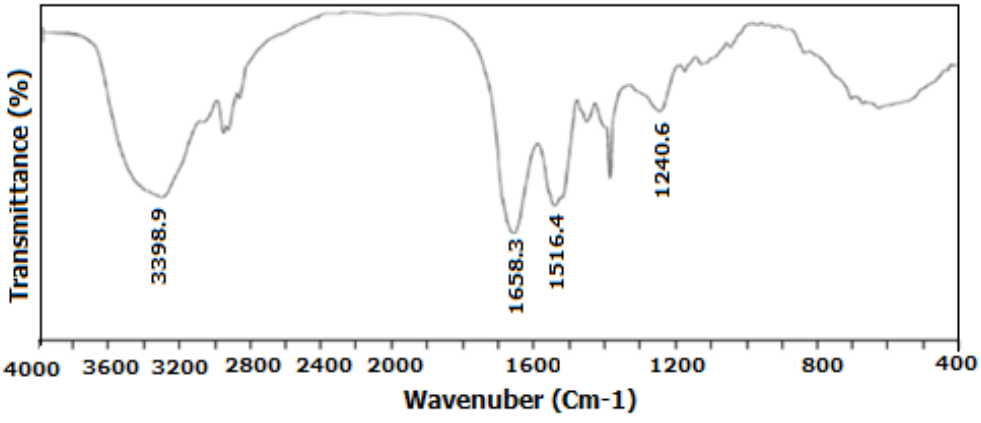

Fig. 1. Infrared spectra of human insulin

2.2 Adsorbent

The calcium-deficient hydroxyapatite (CDHA) powders were prepared at room temperature by a simple co-precipitation method between two solution A and B.[21] The solution A [0.15 mol of calcium nitrate $Ca(NO_3)_2{\cdot}4H_2O$ (Riedel- de Haën - Germany) in 500 mL of distilled water] was added quickly to the solution B [0.26 mol of di-ammonium hydrogenphosphate $(NH4)_2HPO_4$ (Riedel-de Haën, Germany) in 1000 mL of distilled water]. The pH of the mixture obtained was adjusted 7 by ammoniac solution. After stirring for 2 h at the speed of 250 trs/min, the precipitate was filtered, washed, and dried at 343 K for 48 h.

2.3 Experimental protocol

2.3.1 Adsorption measurements

To examine the adsorption capacity of the adsorbent, experiments were carried out by adding 20 mg of powder hydroxyapatite in1ml of insulin in a conical test tube (5 ml capacity). After stirring for 1 min (1000 rpm), the samples were placed in a thermostatic bath at 310 K for different contact times. Then, the solid was separated from the solution by the fritted glass (Frit Glass N°4). The collected solids were dried in the oven at 343 K for 24 h and solutions were stored at 277 K. The solutions were examined by measuring the pH and determining the equilibrium concentration using a UV–vis spectrophotometer (Model 3100, Japan) at 540 nm. The amount adsorbed at equilibrium $q_e(mg/g)$ of insulin by the apatite was determined from the relation :

$$q_e = V \times (\Delta C)/W \quad (1)$$

where $V(l)$ is the volume of solution in contact with the mass $W(g)$ of apatite, and $\Delta C(mg/ml)$ is the difference between the initial (C_0) and final (C_e) equilibrium concentrations. The adsorption rate was calculated from the relation:

$$\%ads = (\Delta C/C_0) \times 100 \quad (2)$$

The values of the adsorption of insulin by the hydroxyapatite in triplicate samples were reproducible within accuracies of ~5%.

2.3.2 Release measurements

Release studies of insulin were investigated by batch experiments. A 20 mg of hydroxyapatite previously adsorbed of the insulin was added in 1ml of physiological saline (NaCl 9 g/L). After stirring for one 1min (1000 rpm), the mixture was placed in a thermostatic bath at 310 K. Finally, the solid and solution were separated by fritted glass (Frit Glass N°4).

The amount released $q_{rel}(mg/g)$ of insulin from hydroxyapatite was calculated by the equation :

$$q_{rel} = C_{rel} \times V/W \quad (3)$$

where $C_{rel}(mg/l)$ is the equilibrium concentration, and $V(l)$ is the volume of solution in contact with the mass $W(g)$ of apatite. The percentage of insulin release was determined from the relation:

$$\%rel = (q_{rel}/q_e) \times 100 \quad (4)$$

The values of the release in triplicate samples were reproducible within accuracies of ~5%.

3. Results and discussion

3.1 Physico-chemical characterization of the adsorbent (CDHA)

3.1.1 Chemical Analyses

The calcium ion content was determined by complexometric titration with Ethylene Diamine Tetra Acetic Acid (EDTA). The quantity of matter of calcium in CDHA varied from 0.812 to 0.822 mol with a mean value of 0.817 ± 0.005mol. The phosphorus content was determined by spectrophotometric method using phosphovanadomolybdic acid with GBC UV-Visible spectrophotometer 911A at 460 nm. The quantity of matter obtained in CDHA varied from 0.509 to 0.519 mol with a mean value of 0.514 ± 0.005 mol. The mean value obtained of Ca/P molar ratio of powder is 1.59 ± 0.01, it is between 1.5 and 1.67. This value obtained is about 8 % below the stoichiometric value of 1.67, which indicates the synthesis of Ca-deficient hydroxyapatite (CDHA).

3.1.2 Surface Area

The specific surface area was determined according to the triple-point BET (Brunauer, Emmett, Teller) method using N_2 adsorption.[22] The value found of the CDHA powder is about 137 ± 0.05 m^2/g, it is higher than ~75 m^2/g of the stoichiometric HA prepared under the same experimental conditions. This high specific surface area can improve the interaction performance of adsorbates to CDHA.

3.1.3 Point of zero charge determination pH_{ZPC}

The point of zero charge is one of the most important parameters used to describe variable-charge surfaces. The apatite surface can bear net positive, negative, or no charge. The pH_{ZPC} corresponds to the equality between the negative charges and the positive charges on the surface of a solid in contact with a polar liquid phase.[23] At pH values below pH_{ZPC}, the CDHA surface is positively charged and will mainly retain anions, while at pH above pH_{ZPC} the surface of CDHA is

negatively charged and predominantly exhibit an ability to exchange cations. The zero-point charge is measured using a simple technique. Briefly, to a series of beakers, 20mL of 0.01 M NaCl solution is added to 0.2 g of apatite powder and the initial pH is adjusted by using HCl (0.1 M) or NaOH (0.1 M) solution in the range of 4–10. After 48 hours of stirring speed (250 rpm) at ambient temperature, the final pH is measured. In order to determine the pH_{zpc}, the difference between the final and initial pH ($\Delta pH = pH_f - pH_i$) is plotted against the initial pH (pH_i). The intersection of ΔpH with the axis $pH_f = pH_i$ is the pH_{ZPC} of the apatite. In the present study, the pH_{ZPC} of the CDHA of Ca/P=1.59 is found to be 5.6 (**Fig. 2**).

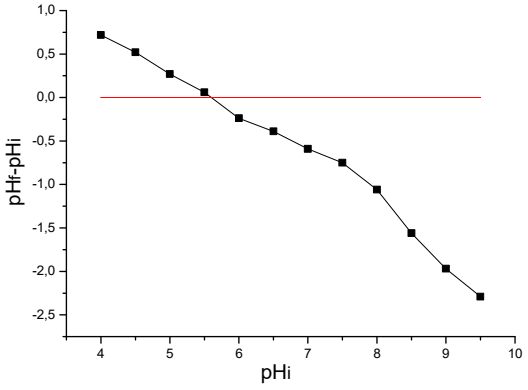

Fig. 2. pH_{ZPC} of CDHA precipitate at room temperature

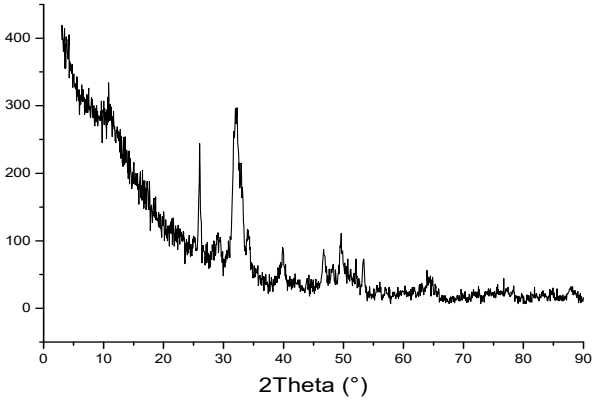

Fig. 3. XRD of CDHA precipitate at room temperature

3.1.4 X-Ray Diffraction Pattern

The X-ray diffraction (XRD) pattern was conducted using an X-ray diffractometer X'PERT PRO with Cu-Ka radiation at room temperature. The apatite yielded broad and overlapping reflections, indicating their poor crystallinity (**Fig.3**).

3.1.5 Infrared spectrum

Infrared spectroscopy IR was carried out after dispersion of anhydrous KBr (about 2 mg product to 200 mg of KBr) using VERTEX 70/70v FT-IR spectrometers. The spectrum obtained in the range of 4000–400 cm^{-1} shows characteristic main peaks of functional groups PO_4^{3-}, OH^- and HPO_4^{2-} of calcium phosphate prepared (**Fig. 4**). The FTIR absorption peak positions and their corresponding assignments are collected in **Table 2**. The peaks observed at 875, 900 and 2984 cm^{-1} are attributed to the HPO_4^{2-} groups.[24,25] The presence of these ions in small quantities, substituted for the PO_4^{3-} groups, attests that the prepared apatite is slightly non-stoichiometric and of low crystallinity.

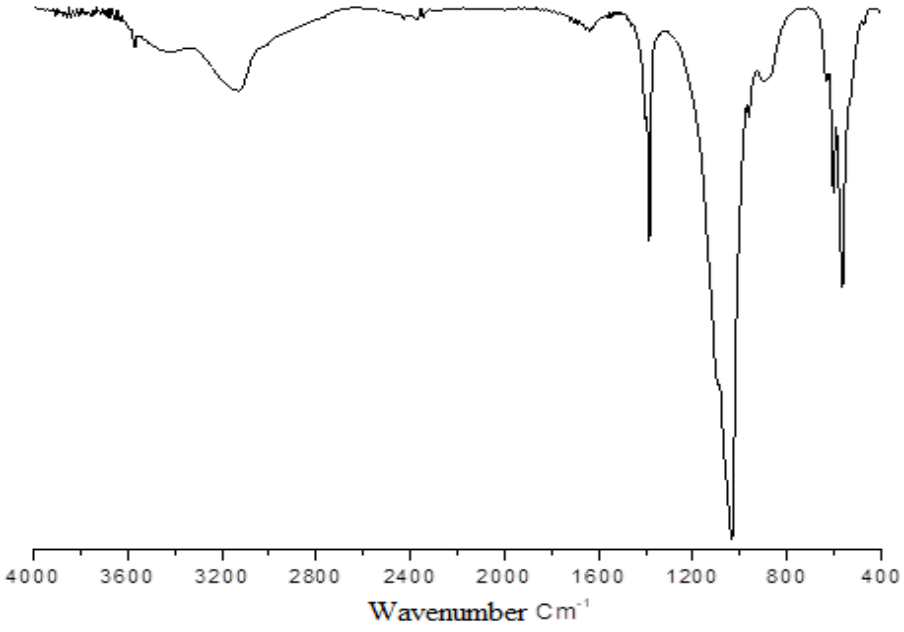

Fig. 4. FTIR spectra of the CDHA precipitate at room temperature

Table 2. FTIR absorption peak positions of prepared CDHA and their corresponding assignments.

Peak position, cm^{-1}	Corresponding assignment
3570, 633	OH-
2984, 901, 875	HPO_2^{4-}
3000-3400, 1638, 312	H_2O
1034, 962	phosphate stretching vibration PO_3^{4-}
600, 564, 474	phosphate bending vibration PO_3^{4-}

3.2 Adsorption of insulin to CDHA

3.2.1 Adsorption kinetics

The kinetic experiments were carried out for different contact times (0, 15, 30, 60, 180, 300,480 and 1440 min) with constant adsorbent dose (20 mg), initial concentration (Co =3500 mg/L), pHi (7.0 –7.2) and at 310 K. The evolution of the amount of insulin adsorbed as a function of incubation time is shown in **Fig.5**. The equilibrium was quick; in fact, the maximum adsorption was reached in the first half-hour of contact, this can be explained by the high number of active sites available in CDHA at the beginning of the adsorption process. The result showed that the adsorption rate reached up to 81±5%. It was observed that the pH values of supernatant solutions after adsorption are between 5.95 and 7.00 ±0.05 (**Fig.6**), which shows it depends on the contact time of adsorbate-CDHA. Moreover, these values are higher than the isoelectric point (pI)= 5.4 ±0.05 of insulin, and also are above the pHpzc of CDHA, which indicates their anionic states. The slight decrease of the pH over time may be explain to the protonation of CDHA surface caused by their frequent interaction with insulin which have the tendency to release H^+ protons and surround the surface of the adsorbent.

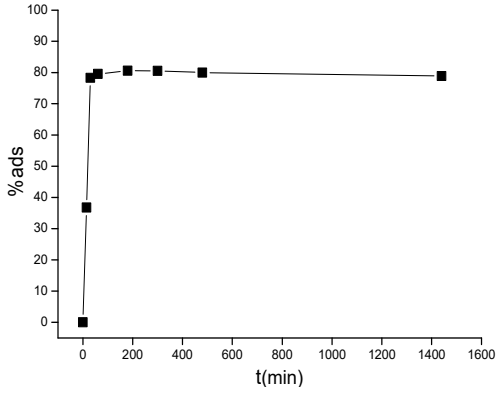

Fig. 5. Kinetics of adsorption of insulin on CDHA of Ca/P= 1.59 (solid quantity : 20 mg, initial insulin concentration : 3500 mg/L, initial pH, at 310 K, stirring time : 1 min)

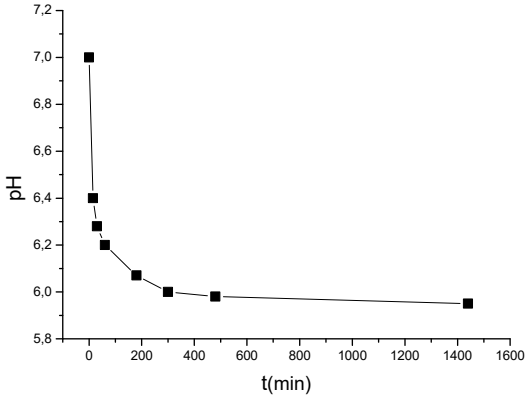

Fig. 6. pH of supernatant solutions after adsorption of insulin onto CDHA of Ca/P= 1.59 (Co = 3500 mg/L) at 310 K.

In order to identify the rate, kinetic parameters and reaction mechanism controlling the adsorption of insulin by hydroxyapatite, five simplified kinetic models namely pseudo first-order,[26] pseudo second-order,[27] Elovich equation,[28] Weber and Morris intraparticle diffusion model[29] and Bangham's pore diffusion model[30] have been evaluated.

3.2.1.1 pseudo-first-order model

The pseudo first order kinetics model is the first equation for the sorption of liquid/solid system described by the Lagergren equation :

$$dq_t/dt = K_1(q_e - q_t) \quad (5)$$

After applying the initial conditions ($q_t = 0, t = 0$), the integration of this equation leads to the following linear form:

$$Ln(q_e - q_t) = Lnq_e - K_1 t \quad (6)$$

Where, $q_e(mg\ g^{-1})$ represents the amount of insulin adsorbed onto CDHA at equilibrium, $q_t(mg\ g^{-1})$ represents the amount of insulin adsorbed at any time t (min) and $K_1(min^{-1})$ represents the rate constant of pseudo first order reaction.

The constant K_1 and theoretical equilibrium adsorption capacity $q_e(Cal)$ calculated from straight-line plot of $Ln(q_e - q_t)$ versus t (**Fig.7**), are given in **Table3**. We noted that the values of the calculated $q_e(Cal)$ and experimental q_e(exp) were different. Moreover, the value of R^2 correlation coefficient (0.951) was less to unity. Therefore, the adsorption of insulin on the CDHA do not follow the pseudo-first-order kinetic model.

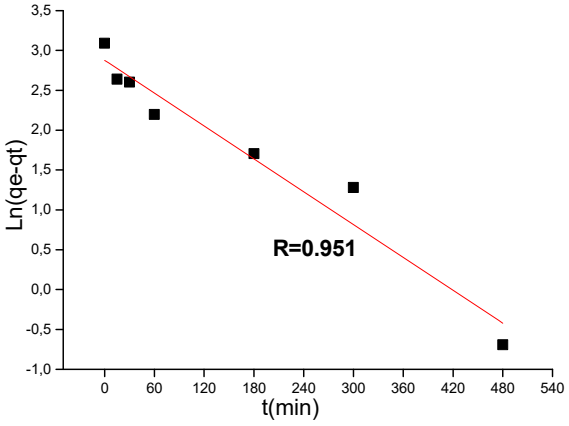

Fig. 7. Pseudo-first-order kinetic for adsorption of insulin on CDHA of Ca/P=1.59

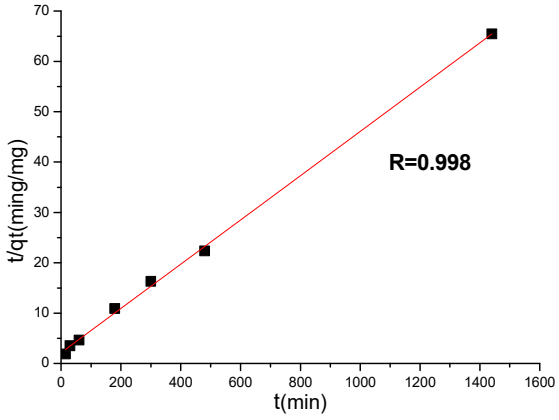

Fig. 8. Pseudo-second-order kinetic for adsorption of insulin on CDHA of Ca/P=1.59

3.2.1.2 pseudo-second order model

The kinetic expression of the pseudo second order model, proposed by Ho and McKay is given by the equation:

$$dq_t/dt = K_2(q_e - q_t)^2 \quad (7)$$

After integration and applying boundary conditions, $t = 0$ to $t = t$ and $q_t = 0$ to $q_t = q_t$; this equation can be written as:

$$t/q_t = 1/K_2.q_e^2 + t/q_e \quad (8)$$

where, $K_2(g/mg.min)$ is the rate constant of pseudo second order reaction. The values of K_2 and $q_e(Cal)$ (**Table 3**) were calculated from the slope and intercept of straight portion of the linear plots obtained by plotting t/q_t against t (**Fig. 8**).

The initial adsorption rate $g(mg/g\ min)$, is calculated at $t \to 0$ from the relationship:

$$g = K_2.{q_e}^2 \quad (9)$$

The correlation coefficient value (0.998) was very high and close to unity, and the $q_e(Cal)$ (22.37 $mg.g^{-1}$) calculated by using the second order model was nearly equal to the q_e(exp) (22 $mg.g^{-1}$) obtained experimentally.

The adsorption reaction of insulin on the surface of CDHA starts from the first minutes of contact, indicating that the most influential and rate-limiting step of the kinetic process is likely to be the pseudo-second order, which controls at each instant t the rate of reaction of insulin transfer.

3.2.1.3 Elovich model

This model is widely used to describe the chemical adsorption of adsorbate molecules on the surfaces of solids of very heterogeneous adsorbents. The kinetic expression of the Elovich model is given by the following equation:

$$dq_t/dt = \alpha.exp(-\beta.q_t) \quad (10)$$

The integration of this relationship leads to the following linear form:

$$q_t = Ln(\alpha.\beta)/\beta + Ln(t)/\beta \quad (11)$$

where $\alpha(mg/g.min)$ is the initial adsorption rate and $\beta(g/mg)$ is the adsorption constant related to the extent of surface coverage and activation energy for chemisorption. The two kinetic constants will be deemed from the slope and the intersection of the straight line giving q_t as a function of Lnt (**Fig.9**).

From **Table 3**, the correlation coefficient (0.957) is lower than pseudo-second order model, the Elovich kinetic model did not provide a good fit to the experimental data but it shows that the chemisorption, which generally happens by ion exchange, can be the rate-determining step during adsorption of insulin onto CDHA.

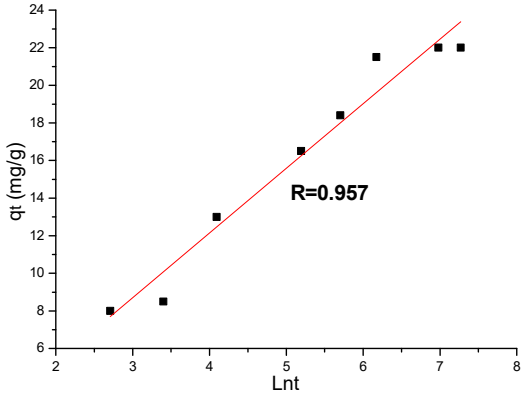

Fig. 9. Plot of Elovich equation for adsorption of insulin onto CDHA of Ca/P=1.59

3.2.1.4 Intra-particle diffusion model

In order to explain the diffusion mechanism, the intra-particle diffusion model proposed by Weber and Morris, was applied to the kinetic data with the pore diffusion factor defined by the following equation:

$$q_t = K_p t^{1/2} + C \quad (12)$$

where, K_p and C are an intra-particle diffusion rate constant($mg.g^{-1}.min^{1/2}$) and a constant, respectively. The K_p and C parametres obtained from the plot of q_t versus $t^{1/2}$ (**Fig.10**), are given in **Table 3**. The rate constant K_p is directly evaluated from the slope of the regression line and C is the value of intercept which gives an idea about the thickness of the boundary layer.

The plot of q_t versus $t^{1/2}$ (**Fig.10**) is not linear over the whole time interval, it shows three *successive* linearities, which indicates that the adsorption is affected by three steps. The first (**1**) is instantaneous adsorption at the external surface of the solid. The second (**2**) is the gradual adoption stage where the intraparticle diffusion is limiting and the third step (**3**) is the final stage before equilibrium (plateau) where the intraparticle diffusion starts to slow down due to the low concentration of the solute in solution.

From **Fig.10** and **Table 3**, the value of C obtained is not zero (q_t versus $t^{1/2}$ plot does not pass through the origin) and the value of the R^2 regression coefficient (0.787) is not satisfactory, indicating that the intra-particle diffusion is not a limiting step but not negligible step in the process of adsorption of insulin on CDHA, especially after the first 30 minutes.

The K_P and C parameters values (**Table 4**) of the Weber and Morris model for three linear portions (**1**), (**2**) and (**3**) show that they evolve over time, we notice a decrease in the value of the diffusion rate constant intraparticle which passes from 1.336 for step (**1**) to $0.0335\ mg.g^{-1}.min^{0.5}$ for step (**3**) and an increase in the value of the ordinate at the origin which passes from 2.214 for the first stage to $20.798\ mg/g$ for the 3rd stage. We also notice that the 2nd step is the only step that presents a good correlation coefficient $R^2(0.995)$ which indicates that this step is the step determining the speed of intraparticle diffusion. Therefore, the intraparticle diffusion process is governed by the second part of the Webber-Morris diagram.

Table 4. Weber and Morris model parameters and correlation coefficients for different stages.

Stage	$K_P(mg.g^{-1}.min^{0.5})$	$C(mg/g)$	R^2
(1)	1.336	2.214	0.785
(2)	0.5915	8.4194	0.995
(3)	0.0335	20.798	0.807

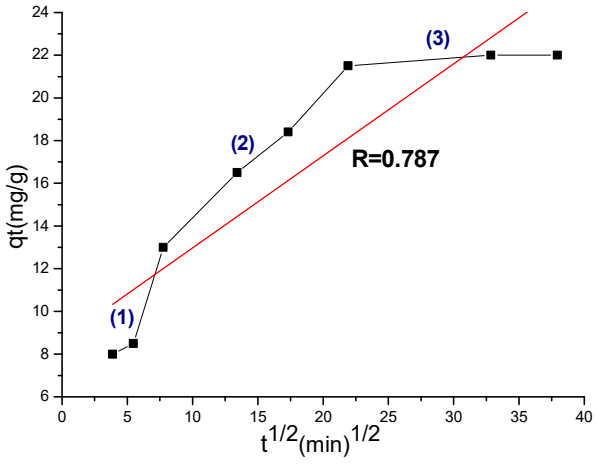

Fig. 10. Intra-particle diffusion model plot for adsorption of insulin on CDHA of Ca/P=1.59

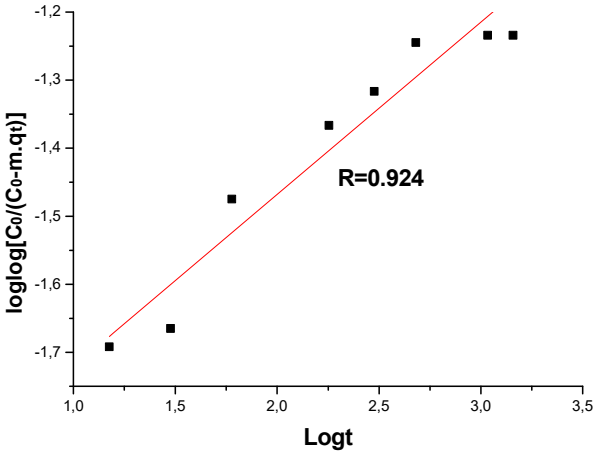

Fig. 11. Bangham's kinetic model plot for adsorption of insulin on CDHA of Ca/P=1.59

3.2.1.5 Pore diffusion model (Bangham's model)

Bangham's kinetic model is applied to evaluate and confirm further the dominance of pore diffusion during the adsorption process. It is defined by the following equation:

$$loglog[C_0/(C_0 - m.q_t)] = \log(m.K_B/2.303V) + \sigma.logt \quad (13)$$

where $q_t(mg/g)$ is the amount of insulin adsorbed at time t, $C_0(mg/L)$ is the initial concentration of the adsorbate in solution, $m(g/L)$ is the mass of the adsorbent, $V(mL)$ is the volume of the solution. $K_B(mL/g.L^{-1})$ and σ (less than 1) are the constants.

The plot of $loglog(C_0/(C_0 - m.q_t))$ against $logt$ (**Fig.11**) was found to be linear with a satisfactory correlation coefficient R^2(>0.9), which confirmed the validity of the kinetics Bangham equation. Therefore the adsorption of insulin onto hydroxyapatite was pore diffusion controlled. The values of K_B and σ (**Table 3**), are calculated from the intercept and slope of the linear plot, respectively.

Table 3. Parameters for various kinetic models for insulin adsorption on CDHA at 310 K, initial insulin concentration 3500 mg/L, pH ≈7 and adsorbent dose 20 mg.

Kinetic models	**Parameters**	
Pseudo-first order	$K_1(min^{-1})$	6.87 10^{-3}
	$q_e(cal)(mg/g)$	17.77
	$q_e(exp)(mg/g)$	22
	R^2	0.951
Pseudo-second order	$K_2(g/mg\ min)$	9.12 10^{-4}
	$q_e(cal)(mg/g)$	22.37
	$q_e(exp)(mg/g)$	22
	$g(mg/g.min)$	0.456
	R^2	0.998
Elovich equation	α(mg/g. min)	2.156
	β(g/mg)	0.291
	R^2	0.957
Intra-particle diffusion	$K_P(mg.g^{-1}.min^{0.5})$	0.417
	$C(mg/g)$	8.914
	R^2	0.787
Bangham's model	$K_B(mL/g.L^{-1})$	1.22 10^{-3}
	σ	0.253
	R^2	0.924

Among the five kinetic models, the pseudo-second-order model generates the best fit for the experimental data. The R^2correlation coefficient obtained is greater than 0.99, indicating that this model is potentially used as a kinetic model of insulin adsorption on the CDHA. Nevertheless, the results shown in **Table 3** do not necessarily mean that the other models are not controlling the rate of the adsorption process, it is generally complex with more than one mechanism limiting the rate of reaction.

3.2.2 Adsorption isotherms

To understand an adsorption process, it is necessary to study adsorption equilibrium and determine the mathematical description best fits the experimental data. For this reason, many adsorption isotherms models are applied. In the present study, four isotherm models have been assessed : the Langmuir,[31] the Freundlich,[32] the Temkin[33] and the Dubinin-Raduskevich[34] models. The variation of the quantity q_e(mg/g) adsorbed of insulin on CDHA as a function of its equilibrium concentration C_e (mg/L) is represented in **Fig.12**. The quickly increases of this quantity for low equilibrium concentrations and then reaching a plateau can be explained by the formation of a monolayer adsorption type.

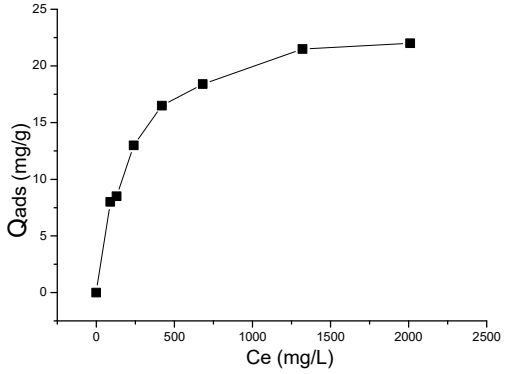

Fig. 12. Adsorption isotherms of insulin by CDHA of Ca/P=1.59 (solid quantity : 20 mg, stirring time : 1 min, T : 310 K)

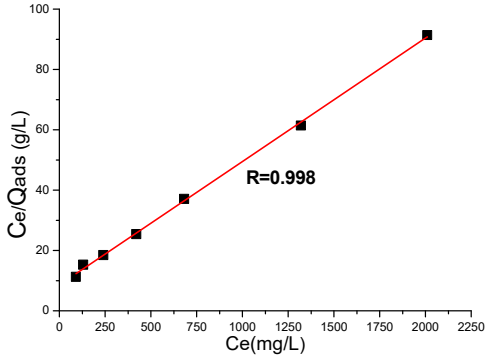

Fig. 13. Langmuir isotherm model

Langmuir isotherm

The Langmuir isotherm is developed on the assumption that the energetic properties of the adsorption sites are uniform and finite. There is no interaction between the molecules adsorbed on neighboring sites. Once the adsorbate is attached to the site, saturation is reached beyond which no further adsorption takes place, which assumes that a monolayer of the adsorbate is formed. The Langmuir equation is given by the following equation:

$$q_e = \frac{q_m K_L C_e}{1+K_L C_e} \tag{14}$$

where q_e is the amount of adsorbate per unit mass of adsorbent (mg/g), K_L is the Langmuir constant related to adsorption capacity (L/g), q_m is the maximum adsorption capacity (mg/g) and C_e is the concentration of adsorbate at equilibrium (mg/l). The linear form of this expression is given by equation:

$$\frac{C_e}{q_e} = \frac{1}{K_L q_m} + \frac{C_e}{q_m} \tag{15}$$

The plot of C_e/q_e versus C_e at 310 K is given in **Fig.13**. The q_m and K_L parameters of Langmuir adsorption are calculated by linear regression and listed in **Table 5**. The results of the Langmuir isotherm model showed a good fit to the experimental data R^2 (0.998) with the equilibrium adsorption capacity found to be 24.46 mg/g.

To evaluate the favorability of the adsorption process, the dimensionless constant separation factor or equilibrium parameter R_L was calculated according to the following equation : [35]

$$R_L = \frac{1}{1 + K_L C_0} \tag{16}$$

where C_0 is the initial concentration of adsorbate (mg/l) and K_L is the Langmuir constant (l/g). R_L values indicate the adsorption to be favorable when $0 < R_L < 1$, unfavorable when $R_L > 1$, linear when $R_L = 1$and irreversible when $R_L = 0$. The R_L values are less than 1 (**Table 4**), indicating that the adsorption of insulin onto the surface of the CDHA was a favorable process at physiological temperature.

Table 4. Dimensionless separation factor (R_L) values for insulin adsorption by CDHA at 310 K.

Insulin concentration (mg/L)	R_L
90	0.701
130	0.619
240	0.468
420	0.334
682	0.236
1320	0.138
2010	0.095

In order to prove nature of the adsorption process, the free energy thermodynamic parameter $\Delta G^0_{ads}(J/mol)$ of adsorption was calculated by the following equation: [36]

$$\Delta G^0_{ads} = -R\ T\ Ln\ K_L \quad (17)$$

where K_L (L/g) is the Langmuir constant, R is the universal gas constant ($8.314\ J\ mol^{-1}K^{-1}$) and T is the absolute temperature in Kelvin. At 310 K, the value found of ΔG^0 (**Table 5**) is in the order of - 4.01, it's negative and between −20 KJ/mol and 0 KJ/mol which indicates that the insulin adsorption is considered a spontaneous process and is often as physical type (physisorption).[37]

Freundlich isotherm

The Freundlich isotherm is developed on the assumption that the adsorption occurs on heterogeneous sites with a non-uniform distribution of energy levels. This model is not restricted to the formation of a monolayer of the adsorbate (multilayer adsorption). The Freundlich equation is commonly given by :

$$q_e = K_F\ C_e^{\frac{1}{n}} \quad (18)$$

where q_e is the amount of adsorbate per unit mass of adsorbent (mg/g), C_e is the equilibrium concentration of adsorbate (mg/L), K_F is the Freundlich constant relative to the adsorption capacity of adsorbent (mg/g) and n is a heterogeneity parameter relative to the adsorption intensity. The exponent $(1/n)$ provides an indication of the favorability and capacity of the adsorbent/adsorbate system.

The linear form of this expression is given by equation:

$$Ln(q_e) = Ln(K_F) + \frac{1}{n}Ln(C_e) \quad (19)$$

Plotting $Ln(q_e)$ versus $Ln(C_e)$ results in a straight line of slope $1/n$ and intercept $Ln(K_F)$ (**Fig. 14**). The values of K_F, n, $1/n$ and the coefficient of determination, R^2, are shown in **Table 5**.

In order to recognize the favorability of the adsorption process and describe the heterogeneity of the adsorption surface, the parameter n must be calculated. The n value between 1 and 10 indicates a favorable process and the value of $1/n$ less than unity indicates a more heterogeneous surface.[38] In the current study, the values obtained for n and $1/n$ are 2.86 and 0.35 respectively, indicating that the adsorption of insulin onto CDHA is favorable and possible to realize on heterogeneous surfaces.

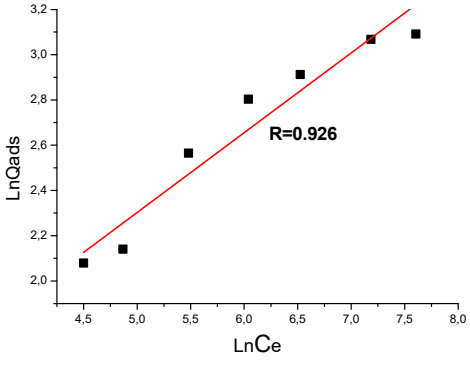

Fig. 14. Freundlich isotherm model

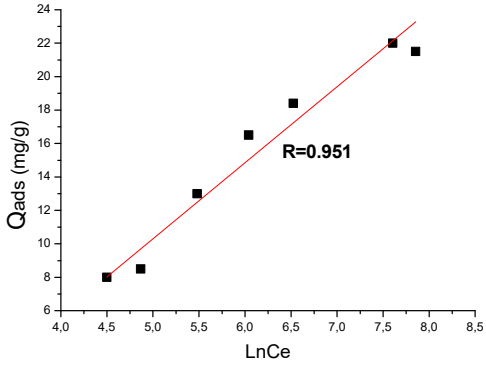

Fig. 15. Temkin isotherm model

Temkin isotherm

Contrary to the Langmuir and Freundlich isotherms, the Temkin model takes into account the interactions between adsorbent and adsorbate and is assumed that the heat of adsorption (ΔH_{ads}) of all molecules in the layer decreases linearly with increased surface coverage. The linear form of the Temkin isotherm can be described by the following equation:

$$q_e = (R\ T/b_t)\ Ln\ a_t + (R\ T/b_t)\ Ln\ C_e \quad (20)$$

where q_e is the amount of adsorbate per unit mass of adsorbent (mg/g), C_e is the equilibrium concentration of adsorbate (mg/L), b_t is the Temkin isotherm constant associated to the heat of adsorption (J mol^{-1}) and a_t is the Temkin isotherm constant corresponding to the maximum binding energy (L/g), R is the universal gas constant (8.314 J mol^{-1} K^{-1}) and T is the temperature at 310 K.

The constants b_t and a_t are determined from the slope and intercept of the linear plot of q_e versus $Ln\ C_e$ (**Fig.15**). The Tamkin model parameters are presented in **Table 5**. The a_t and b_t values are 0.074 L/mg and 0.589 KJ/mol, respectively.

The b_t value is positive, implying an exothermic adsorption reaction. Additionally, the low value of this parameter b_t, suggesting physical interaction between insulin and CDHA.

Dubinin– Kaganer–Radushkevich isotherm

The Dubinin– Kaganer–Radushkevich (D-K-R) model is generally suitable for intermediate- range of adsorbate concentrations with multilayer and microporous solids involving Van Der Waal's forces, applicable for physical adsorption processes. This model is applied to express the adsorption mechanism with Gaussian energy distribution onto heterogeneous surfaces. It is usually applied to differentiate between physical and chemical adsorption. The model is represented by the empirical equation below:

$$q_e = q_D exp(-B_D\ \mathcal{E}^2) \tag{21}$$

where q_e is the amount of adsorbate per unit mass of adsorbent (mg/g), q_D is the maximum adsorption capacity representing the total specific micropore volume of the adsorbent and $B_D(mol^2/J^2)$ is the D-K-R model constant related to mean adsorption free energy $E(KJ/mol)$ per molecule of adsorbate as it migrates to the surface of the adsorbent from infinite distance in the solution. This energy is expressed by:

$$E = 1/\sqrt{2\ B_{DR}} \tag{22}$$

The Ɛ is the Polanyi potential can be calculated as:

$$\mathcal{E} = R\ T\ Ln(1 + 1/C_e) \tag{23}$$

where R and T represent the gas constant $(8.314\ J/mol.K)$ and absolute temperature$(310\ K)$, respectively.

The linearized form of the D-K-R model is given by the following equation:

$$Ln\ q_e = Ln\ q_D - B_D\ \mathcal{E}^2 \tag{24}$$

The slope of the plot of $Ln\ q_e$ versus $\mathcal{E}^2$ gives B_D and the intercept yields the adsorption capacity, q_D (**Fig.16**). The calculated values of B_D, q_D and E are, respectively, $1.23\ 10^{-3} mol^2/J^2$ and $18.28\ mg/g$ and $20.16\ J/mol$ (**Table 5**). The value of E is used to describe the type of adsorption; the E values range from 1.0 to 8.0 KJ/mol for physical adsorption and from 9.0 to 16.0 KJ/mol for chemical adsorption.[39] In the present study, the adsorption energy obtained is less than 8 KJ/mol indicating that the adsorption of insulin onto CDHA may be attributed to the physical adsorption mechanism at the temperature of 310 K. From **Table 4**, the coefficient of regression value is low (0.752) indicating that this model does not simulate the data experimental well, it is not considered as Dubinin– Kaganer–Radushkevich isotherm model preferred.

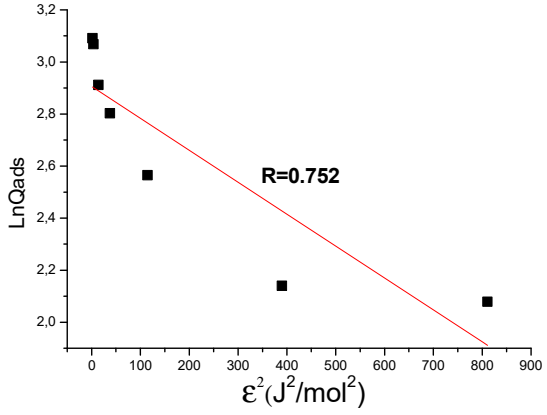

Fig.16. Dubinin – Radushkevich isotherm model

Table 5. Values of the parameters of Langmuir, Freundlich, Temkin and Dubinin–Radushkevich models for the adsorption of insulin onto CDHA of Ca/P=1.59 at 310 K.

Models	Parameters	
Langmuir	K_L(L/g)	4.74
	q_m(mg/g)	24.46
	R^2	0.998
	$\Delta G^0_{ads}(KJ/mol)$	- 4.01
Freundlich	K_F(mg^{1-m} g^{-1} l^m)	1.74
	$1/n$	0.35
	n	2.86
	R^2	0.926
Temkin	b_t(J mol^{-1})	589.35
	a_t(L/g)	0,074
	R^2	0.951
Dubinin–Kaganer–Radushkevich (D-K-R)	E(J.mol^{-1})	20.16
	B_D(mol^2/J^2)	1,23.10^{-3}
	q_D(mg/g)	18,28
	R^2	0.752

Owing to the results of **Table 5**, the Langmuir model appears to be the most appropriate isotherm for the fit of the equilibrium experimental data of adsorption of insulin on the apatitic calcium deficient hydroxyapatite as compared to, Freundlich, Temkin, and Dubinin-Radushkevich models indicating the possibility of the validity of this model under the concentration range studied.

3.2.3 Solid (FTIR)

In order to identify the fixation of the insulin on the synthetic apatitic calcium deficient hydroxyapatite (CDHA), Fourier transform infrared spectrophotometry is used before and after adsorption in 3500 mg/l of insulin in 18 h of contact time (**Fig. 17 and 18**).

The infrared IR absorption spectra obtained before and after insulin adsorption reveal the presence of bands characteristic of the peptide bond of insulin. The band around 1543 cm^{-1} is attributed to the valence vibration of the N-H bond (of the secondary amide). The band located around 1659 cm^{-1} is associated with the elongation of the carbonyl group C=O of the amides. There is also an absorption band located around 3400 cm^{-1} attributable to the stretching vibration of the NH_2 group.

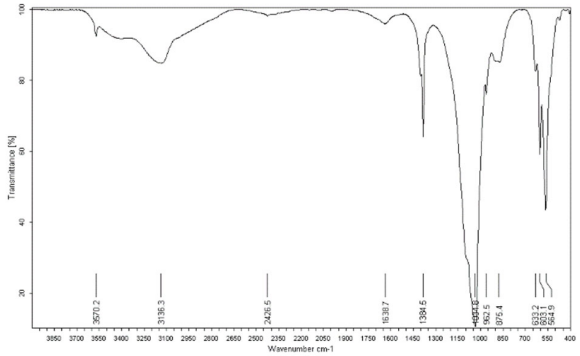

Fig. 17. FTIR spectra of CDHA before adsorption in 3500 mg/L of insulin at 310 K

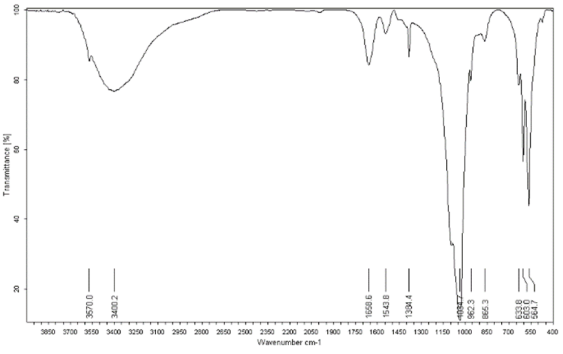

Fig. 18. FTIR spectra of CDHA after adsorption in 3500 mg/L of insulin at 310 K

3.3 Release of insulin by CDHA

In order to examine the effect of time on the release process of insulin previously adsorbed onto the CDHA of Ca/P=1.59, a series of experiments was used for contact times of 0.25 to 24 hours in physiological solution (9g/l NaCl) at 310 K. **Fig. 19** shows a gradual increase to about 41 ± 5% followed by a decrease in release rate after about 1 hour of insulin incubation. The pH of the salting-out solutions varies slightly over time, it is between 5.98 and 5.68 ± 0.05 (**Fig. 20**) and above the point of zero charge of CDHA ($pH_{ZPC} = 5.6$). It may vary depending on the rate of insulin release. This can be explained by the protonation followed by deprotonation of the apatite surface caused by their interaction with insulin which has an isoelectric point $pI = 5.4$ lower than the pH of the releasing solutions.

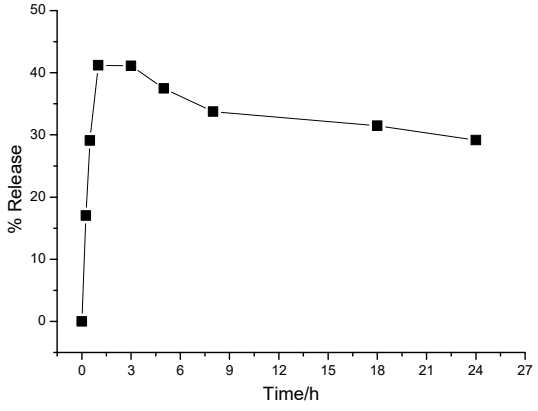

Fig. 19. Rate of insulin released from CDHA of Ca/P 1.59

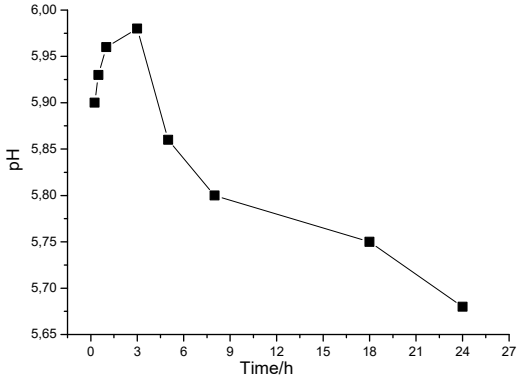

Fig. 20. pH of supernatant solutions after release of the insulin from CDHA

4. Conclusions

The effect of time on the adsorption and release of insulin by synthetic poorly crystalline CDHA of Ca/P =1.59 was examined at 310 K. The result shows that the interaction process was very fast in the first minutes, the decrease in release rate might be explained by the existence of a re-adsorption reaction between the CDHA and insulin previously released in the solution. The adsorption rate is more than that of the release, which can be explained by the high apatite reactivity related to their high specific surface area that can interact with the functional groups of insulin.

Fourier-transform infrared spectroscopy confirms the fixation of insulin by CDHA; the spectra reveal the specific bands of amide I and amide II constituting the peptide bond of the insulin structure.

The pH of the incubation medium of insulin in contact with apatite is more than the point of zero charge ($pH_{ZPC} = 5.6$) of CDHA and the isoelectric point ($pI = 5.4$) of insulin, which shows that the insulin and the CDHA surface are negatively charged. For these reasons, the interaction processes reveal, in this case, an ion exchange involving the replacement of mineral ions of the surface of the apatite (negatively charged functional groups) by insulin molecular ions from the solution. Furthermore, on the surface of CDHA, the functional groups charged negatively are more than the positive groups. Therefore, the interaction process involve the anionic groups of insulin and both the calcium sites and anionic groups of apatite, it is considered a physical interaction.

It appears that the pseudo-second-order kinetic model is the best model to describe the adsorption of insulin onto the CDHA, it can be considered the rate-limiting step which governs the adsorption process. The experimental and calculated maximum adsorption capacities are around $22\ mg\ g^{-1}$ with a high value of the correlation coefficient $R^2(0.998)$. The Langmuir isotherm showed the better fit of all isotherm models studied with a maximum monolayer adsorption capacity of $24.46\ mg\ g^{-1}$ and a high correlation coefficient (0.998). This result suggests that the energetic properties of the adsorption sites of the CDHA are uniform and finite with one molecule of insulin per site, which supposes that a monolayer of the insulin is formed. The parameter values of the isotherm models, such as $\Delta G^0(-4.01KJ/mol)$, $b_t(0.589KJ/mol)$ and $E(0.589KJ/mol)$ can be revealed that the adsorption process is favorable, exothermic, spontaneous in nature, and often controlled by physisorption.

The results obtained show that the synthetic poorly crystalline calcium-deficient hydroxyapatite provides a significant advantage over the interaction induced by insulin. The application of different kinetic models and the adsorption isotherms allows us to analyze successfully the adsorption process, determine the best mathematical model fitting with experimental data, and know the rate-limiting step that governs the overall adsorption rate and its mechanism.

Acknowledgements

The authors would like to express their sincere gratitude to all members of the Laboratory of the Department of Chemistry, for helping and facilitating the realization of this study.

References

1 Billet K., Unlubayir M., Munsch T., Malinowska M. A., de Bernonville T. D., Marchal C., Dedet S., Oudin A., Courdavault V., Besseau S., Giglioli-Guivarc'h N., and Lanoue A. (**2021**) Correction to Postharvest Treatment of Wood Biomass from a Large Collection of European Grape Varieties : Impact for the Selection of Polyphenol-Rich Byproducts. *ACS Sustainable Chem. Eng.*, 9 (9) 3509 -3517.
2 Billet K., Malinowska M. A., Munsch T., Unlubayir M., Adler S., Delanoue G., and Lanoue A. (**2020**) Semi-Targeted Metabolomics to Validate Biomarkers of Grape Downy Mildew Infection Under Field Conditions. *Plants*, 9 (8) 1008.
3 Staszewsky L., Baviera M., Tettamanti M., Colacioppo P., Robusto F., D'Ettorre A., Lepore V., Fortino I., Bisceglia L., Attolini E., Graps E. A., Caldo G., Roncaglioni M. C., Garattini S., and Latini R. (**2022**) Insulin treatment in patients with diabetes mellitus and heart failure in the era of new antidiabetic medications. *BMJ Open Diab. Res. Care*, 10 (2) e002708.
4 Abd-Ella A. A., Metwally S. A., Abd ul-Malik M. A., El-Ossaily Y. A., Abd Elrazek F. M., Aref S. A., Naffea Y. A., and Abdel-Raheem S. A. A. (**2022**) A review on recent advances for the synthesis of bioactive pyrazolinone and pyrazolidinedione derivatives. *Curr. Chem. Lett.*, 11 (2) 157-172.
5 Elhady O. M., Mansour E. S., Elwassimy M. M., Zawam S. A., Drar A. M., and Abdel-Raheem S. A. A. (**2022**) Selective synthesis, characterization, and toxicological activity screening of some furan compounds as pesticidal agents. *Curr. Chem. Lett.*, 11 (3) 285-290.
6 Fouad M. R., Shamsan A. Q. S., and Abdel-Raheem Sh. A. A. (**2023**) Toxicity of atrazine and metribuzin herbicides on earthworms (Aporrectodea caliginosa) by filter paper contact and soil mixing techniques. *Curr. Chem. Lett.*, 12 (1) 185-192.
7 Tolba M. S., Sayed M., Kamal El-Dean A. M., Hassanien R., Abdel-Raheem Sh. A. A., and Ahmed M. (**2021**) Design, synthesis and antimicrobial screening of some new thienopyrimidines. *Org. Commun.*, 14 (4) 334-345.
8 El Rhilassi A., and Bennani-Ziatni M. (**2022**) Experimental study on the interaction of insulin with apatitic calcium phosphates analogous to bone minéral : adsorption and release. *Curr. Chem. Lett.*, 11 (4) 341–352.
9 Kandori K., Masunari A., and Ishikawa T. (**2005**) Study on adsorption mechanism of proteins onto synthetic calcium hydroxyapatites through ionic con- centration measurements. *Calcif Tissue Int.*, 76, 194-206.
10 Ielo I., Calabrese G., De Luca G., and Conoci S. (**2022**) Recent Advances in Hydroxyapatite-Based Biocomposites for Bone Tissue Regeneration in Orthopedics. *Int J Mol Sci.*, 23 (17) 9721.
11 Cheng L., Ye F., Yang R., Lu X., Shi Y., Li L., Fan H., and Bu H. (**2010**) Osteoinduction of hydroxyapatite/ β-tricalcium phosphate bioceramics in mice with a fractured fibula. *Acta Biomater.*, 6 (4) 1569-74.
12 Nawawi N. A., Alqap A. S. F., and Sopyan I. (**2011**) Recent Progress on Hydroxyapatite-Based Dense Biomaterials for Load Bearing Bone Substitutes. *Recent Patents Mater. Sci.*, 4 (1) 63- 80.

13 Oguchi H., Ishikawa K., Mizoue K., Seto K., and Eguchi, G. (**1995**) Long-term histological evaluation of hydroxyapatite ceramics in humans. *Biomater.*16 (1) 33-38.
14 Yoon S. Y., Park Y. M., Park S. S., Stevens R., and Park H. C. (**2005**) Synthesis of hydroxyapatite whiskers by hydrolysis of A-tricalcium phosphate using microwave heating. *Mater. Chem. Phys*., 91 (1) 48- 53.
15 Ota Y., Iwashita T., Kasuga T., and Abe Y. (**1998**) Novel Preparation Method of Hydroxyapatite Fibers. *J. Am. Ceram. Soc.*, 81 (6) 1665- 8.
16 Dorozhkin S. V. (**2011**) Calcium orthophosphates : Occurrence, properties, biomineralization, pathological calcification and biomimetic applications. *Biomatter*., 1 (2) 121-164.
17 Mavropoulos E., Rossi A. M., da Rocha N. C. C., Soares G. A., Moreira J.C., and Moure GT. (**2003**) Dissolution of calcium-deficient hydroxyapatite synthesized at different conditions. *Mater Charact.*, 50 (2-3) 203-207.
18 Drouet C. (**2013**) Apatite formation : why it may not work as planned, and how to conclusively identify apatite compounds. *Biomed. Res. Int.*, 490946, 1-12.
19 Yesilel O. Z., Olmez H., and Arici C. (**2007**) The first bis(orotato-N,O) cadmium complex with monodentate protonated ethylenediamine ligands: Synthesis, spectrothermal properties of a cadmium(II)-orotato complex with ethylenediamine – Crystal structure of trans-[Cd(HOr)2(enH)2]· 2H2O and cis-[Cd(H2O)2(phen)2](H2Or)2·2H2O. *Polyhedron*, 26, 3669-3674.
20 Dorkoosh F.A., Coos Verhoef J., Ambagts M.H.C., Rafiee-Tehrani M., Borchard G., and Junginger H.E. (**2002**) Peroral delivery systems based on super porous hydrogel polymers : release characteristics for the peptide drugs buserelin, octreotide and insulin. *Eur. J. Pharm. Sci*., 15 (5) 433- 439.
21 Rey C., Liam J., Grynpas M., Shapiro F., Zylerberg L., and Glimcher M. J. (**1989**) Non-apatitic environments in bone mineral, FT-IR detection, biological properties and changes in several disease states. *Connect. Tissue Res.*, 21 (1-4) 267-273.
22 Brunauer S., Emmett P. H., and Teller E. (**1938**) Adsorption of Gases in Multimolecular Layers. *J. Am. Chem. Soc.*, 60 (2) 309- 319.
23 Noh J.S., and Schwarz J.A. (**1989**) Estimation of the point of zero charge of simple oxides by mass titration. *J. Colloid Int Sci*., 130 (1) 157-164.
24 Markovic M., Fowler B.O. and Tung M.S. (**2004**) Preparation and Comprehensive Characterization of a Calcium Hydroxyapatite Reference Material. *J. Res. Natl. Inst. Stand. Technol.*, 109 (6) 553- 568.
25 Von Euw S., Wang Y., Laurent G., Drouet C., Babonneau F., Nassif N., Azaïs T. (**2019**) Bone mineral : New insights into its chemical composition. *Sci. Rep.*, 9 (1) 1–11.
26 Lagergren S., and *Svenska* K. (**1898**) About of the *theory of so - called adsorption of soluble substances***.** Vetenskapsakad Handl**,** *24 (2) 1-39***.**
27 Ho Y.S., and McKay G. (**1999**) Pseudo-second order model for sorption processes. *Process Biochem*., 34 (5) 451- 465.
28 Chien S.H., and Clayton W.R. (**1980**) Application of Elovich Equation to the Kinetics of Phosphate Release and Sorption in Soils. *Soil. Sci. Soc. Am. J.*, 44 (2) 265-268.
29 Weber W. J., and Morris J. C. (**1963**) Kinetics of adsorption on carbon from solution. *J. Sanit. Eng. Div., Am. Soc. Civ. Eng.*, 89 (SA2) 31- 40.
30 *Aharoni C.***,** and *Ungarish M.***,** (**1977**) Kinetics of activated chemisorption. Part 2. Theoretical models**.** ***J. Chem. Soc. Faraday Trans., 73, 456-464.***
31 Langmuir I. (**1918**) The adsorption of gases on plane surfaces of glass, mica and platinum. *J. Am. Chem. Soc.*, 40 (9) 1361-1403.
32 Freundlich H. M. F. (**1906**) Über die adsorption in lösungen. *Z. Phys. Chem.*, 57, 385-470.
33 Temkin M. J., and Pyzhev V. (**1940**) Recent modifications to Langmuir Isotherms. Acta. *Physicochimie USSR.*, 12, 217-222.
34 Dubinin M. M., and Radushkevich L. V. (**1947**) Equation of the Characteristic Curve of Activated Charcoal. *J. Proc. Acad. Sci. USSR, Phys. Chem.*, 55, 331-333.
35 Weber T. W., and Chakravorti R. K. (**1974**) Pore and solid diffusion models for fixed-bed adsorbers. *Am. Inst. Chem. Eng. J*., 20 (2) 228-238.
36 Ho Y. S. (**2006**) Isotherms for the sorption of lead onto peat: Comparison of linear and non-linear methods. *Pol. J. Environ. Stud.*, 15 (1) 81–86.
37 Jiang L., Li S., Yu H., Zou Z., Hou X., and Shen F. (**2016)** Amino and thiol modified magnetic multi-walled carbon nanotubes for the simultaneous removal of lead, zinc, and phenol from aqueous solutions. *Appl. Surf. Sci.*, 369, 398-413.
38 Hall K. R., Eagleton L. C., Acrivos A., and Vermeulen T. (**1966**) Pore- and solid-diffusion kinetics in fixed-bed adsorption under constant-pattern conditions. *Ind. Eng. Chem. Fund.*, 5(2) 212-223.
39 Helfferich F. (**1962**) Ion exchange. *McGraw-Hill, New York*, 335-360.